Oscillations modulating power law exponents in isotropic turbulence: Where experiments and simulations agree and differ

Kartik P. Iyer,[1] Gregory P. Bewley,[2] Luca Biferale,[3] Katepalli R. Sreenivasan,[1, 4, *] and P. K. Yeung[5]

[1]*Department of Mechanical and Aerospace Engineering,*
New York University, New York, NY, 11201, USA
[2]*Schools of Aerospace and Mechanical Engineering,*
Cornell University, Ithaca, New York, NY, 14853, USA
[3]*Department of Physics and INFN, University of Rome Tor Vergata, Rome, 00133, Italy*
[4]*Department of Physics and the Courant Institute of Mathematical Sciences,*
New York University, New York, NY 11201, USA
[5]*Schools of Aerospace and Mechanical Engineering,*
Georgia Institute of Technology, Atlanta, GA 30332, USA

Inertial-range features of turbulence are investigated using data from experimental measurements of grid turbulence and direct numerical simulations of isotropic turbulence simulated in a periodic box, both at the Taylor-scale Reynolds number $R_\lambda \sim 1000$. In particular, oscillations modulating the power-law scaling in the inertial range are examined for structure functions up to sixth order moments. The oscillations in exponent ratios decrease with increasing sample size in simulations though, in experiments, they survive at a low value of 4 parts in 1000 even after massive averaging. The two data sets are consistent in their intermittent character but differ in small but observable respects. Neither the scaling exponents themselves nor all the viscous effects are consistently reproduced by existing models of intermittency.

Turbulent fluctuations on scales intermediate between the small scale η and the large scale L, the so-called inertial range, are thought to conform to power-laws [1–4]. In particular, one writes

$$S_m(r) \equiv \langle [\delta_r u]^m \rangle \sim r^{\zeta_m} , \eta \ll r \ll L , \qquad (1)$$

where $\delta_r u = [\boldsymbol{u}(\boldsymbol{r}+\boldsymbol{x}) - \boldsymbol{u}(\boldsymbol{x})] \cdot \hat{\mathbf{r}}$ is the longitudinal velocity increment, m is the moment-order, $\hat{\mathbf{r}}$ is a unit vector along vector $\mathbf{r}$, r denotes magnitude of $\mathbf{r}$ and $\langle \cdot \rangle$ denotes a suitable average. Although the theoretical basis for Eq. 1 exists only for $m = 3$ [5], it is empirically regarded as viable for other orders as well [6]. The power-law scaling of Eq. 1, apart from offering the allure of ubiquity [7–10], often allows a simplification of subsequent analysis (for example, see [11]).

Recently, extensively sampled data from grid turbulence [12] have shown an interesting feature with respect to Eq. 1 (see Fig. 1) that power law exponents may be modulated by undulations that are only partly explained by existing intermittency models [25]. These oscillations become explicit when the exponent ratios ζ_4/ζ_2 in Eq. 1 are examined, as the authors of [12] showed (see Fig. 1). The oscillations decrease with Reynolds number. Here, by examining even more extensive data from the same experiment [12] at one Reynolds number, along with those from direct numerical simulations [13–15] at a comparable Reynolds number, we show that inertial range undulations observed in Fig. 1 manifest in exponent ratios such as ζ_4/ζ_2, in both experiments (EXP) and simulations (DNS), but diminish in the limit of massive averaging; they seem to disappear in simulations to yield pure power-law scaling (Eq. 1), but settle down to very small root-mean-square magnitudes (rms) of the order

	N^3	L/η	ns	R_λ
EXP	–	2567	10^{10}	1030
DNS	8192^3	2514	10^{15}	1300

TABLE I. Parameters of the data from the experiment and direct numerical simulation. N^3 is the number of collocation points for DNS in a periodic cube of fixed size L_0. L/η is the ratio of the integral scale L ($L/L_0 \approx 0.2$ for DNS) to the Kolmogorov scale $\eta \equiv (\nu^3/\langle \epsilon \rangle)^{1/4}$, where ν is the kinematic viscosity, $\langle \epsilon \rangle$ the mean dissipation rate; ns is the total number of samples in space and/or time (but the meaning of ns in EXP and DNS is different because the ratio of the number of independent samples to ns differ between EXP and DNS); R_λ is the Taylor microscale Reynolds number.

of 4 parts in 1000 in the experiment. The situation at higher R_λ is unknown at present. Both EXP and DNS show that the ratios ζ_4/ζ_2 and ζ_6/ζ_2 differ from the classical Kolmogorov phenomenology [1], but differ in small but observable respects between them. We comment on their possible origin.

Table I reports a few important parameters in EXP and DNS. The Reynolds numbers (R_λ) in both EXP and DNS are sufficiently high and comparable to each other. The experiments were run for an unprecedented duration and averages performed over more than 10^5 independent turn-over times of the turbulence, but the averaging is performed for only one component of the velocity and do not take account of possible residual anisotropies; the DNS data, on the other hand, extensive though they are, do not correspond to similarly large number of independent realizations but perform spherical averaging over the solid angle to obtain the isotropic sector [16, 17] by the method given in [18], and eliminates residual anisotropy
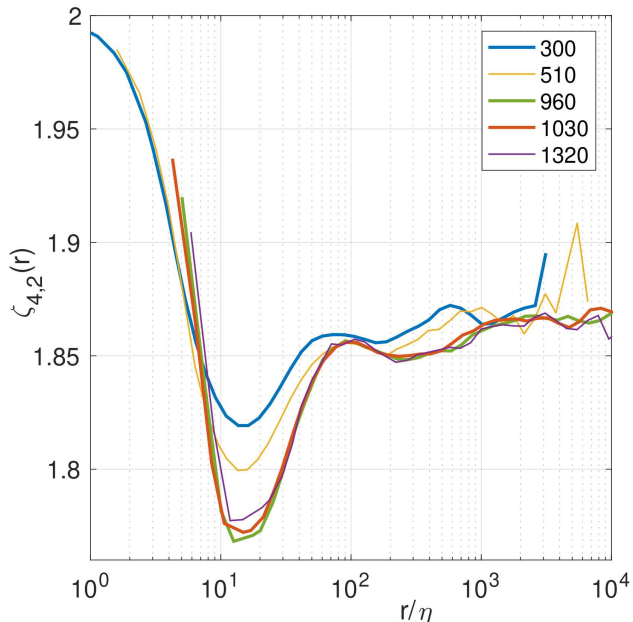
FIG. 1. Replot of data from [12] of the ratio of logarithmic local slopes of fourth order longitudinal velocity structure function (S_4) to the corresponding quantity for the second order (S_2) vs. spatial separation r normalized by Kolmogorov scale (η); see Eq. (2). The two thinner curves were computed from datasets about ten times shorter than the others, as explained in [12]. The legend shows the microscale Reynolds numbers R_λ.

effects.

In order to measure exponents ζ_m in Eq. 1 we consider the logarithmic local slopes of velocity difference moments $S_m(r)$ of order m,

$$\zeta_m(r) \equiv \frac{d \log S_m(r)}{d \log(r)} . \qquad (2)$$

If the moments $S_m(r)$ exhibit proper inertial range scaling according to Eq. 1 then $\zeta_m(r)$ are constants in the inertial range $\eta \ll r \ll L$. In Fig. 2 we compare the ratio of local slopes $\zeta_{4,2} \equiv d[\log S_4]/d[\log S_2] = \zeta_4(r)/\zeta_2(r)$ from EXP and DNS. This is the first non-trivial ratio between exponents of analytic functions that involve no modulus, and is less affected by strong cancellations (as can happen for odd-orders) and poor statistics (as can happen for higher-order moments) [22, 23]. The point of [12] was this ratio had an undulating character in the inertial range, albeit of decreasing magnitude with increasing Reynolds numbers.

Figure 2(a) shows that the general trend in EXP (circles) and the isotropic DNS data (solid line) is very similar with a conspicuous R_λ-dependent viscous dip around $r/\eta \sim 10$ predicted by the multifractal model [24, 25]. With increasing scale-size a crossover "bottleneck" between the viscous and inertial regimes around $r/\eta = 80$
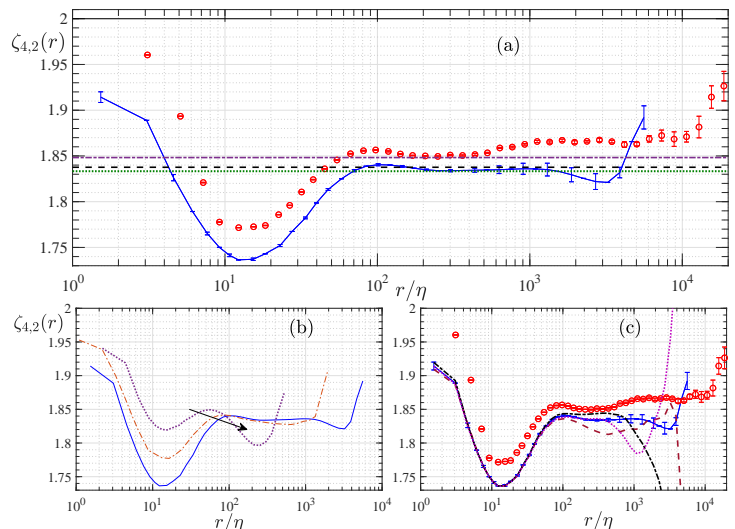

FIG. 2. Ratio of logarithmic local slopes of S_4 and S_2, $\zeta_{4,2}(r) \equiv d[\log S_4(r)]/d[\log S_2(r)]$, versus spatial separation r normalized by Kolmogorov scale η. (a) Data from EXP at $R_\lambda = 1030$ (open circles) are from [12]; the isotropic sector from DNS at $R_\lambda = 1300$ (solid line) [15] are compared with the p-model (dash-dot line) of Meneveau and Sreenivasan [19], She-Leveque model (dashed line) [20] and that by Yakhot (dotted line) [21]. Horizontal line at $\zeta_{4,2} = 2$ corresponds to non-intermittent scaling [5]. Error bars indicate the standard error obtained from temporal fluctuations of local slopes. (b) Isotropic DNS data at different Reynolds numbers: $R_\lambda = 240$ (dotted line), 650 (dash-dot line) and 1300 (solid line) are plotted to show that the viscous bottleneck around $r/\eta = 80$ decreases in amplitude with increasing R_λ in the direction shown. (c) Data from EXP (open circles), compared with the DNS data for the isotropic sector (solid line) and the one-dimensional cuts in DNS along the three Cartesian directions: $\hat{\mathbf{r}} = (1, 0, 0)$ (dotted line), $\hat{\mathbf{r}} = (0, 1, 0)$ (dashed line) and $\hat{\mathbf{r}} = (0, 0, 1)$ (dash-dot line). The latter three illustrate that the inertial range value of $\zeta_{4,2}(r)$ can be affected by non-universal large scale effects when not projecting onto the isotropic sector.

is seen in both EXP and DNS. This is not predicted by any existing models. This viscous bottleneck (which lies outside the inertial range) decreases in amplitude with increasing R_λ as shown in Fig. 2(b) in the DNS (see also Fig. 1). The relation between this physical space bottleneck and that in the Fourier space [26, 27] remains to be understood properly.

It is evident from Fig. 2(a) that inside the inertial range $\eta \ll r \ll L$, which is roughly estimated to be in the range $r/\eta \in (100, 1000)$ [15], $\zeta_{4,2}$ from both EXP and isotropic sector of DNS differ from the self-similar value of $\zeta_{4,2} = 2$ indicating that higher-R_λ turbulence is indeed intermittent with a definite departure from the K41-similarity [5]. One can also see that EXP and isotropic DNS data differ from one another and both show some r-dependent undulations instead of the r-independent constant (see Eq. 1). The finite (and small) mismatch in $\zeta_{4,2}$ between EXP and
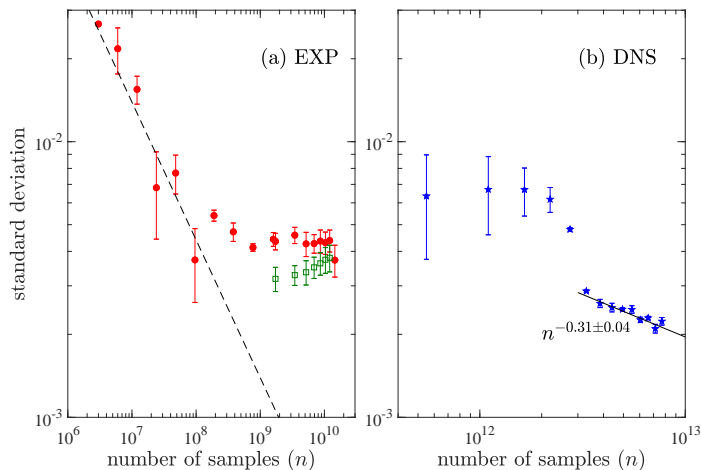
FIG. 3. Log-log plot of the standard deviation of the oscillation amplitude in $d[\log(S_4)]/d[\log(S_2)]$ from its mean value in the range $r/\eta \in (100, 1000)$ in Fig. 2 as function of sample size n for (a) the experiments and (b) the isotropic sector from DNS. Error bars indicate the variation obtained by changing the interval $r/\eta \in [100, 1000]$ by 10% on either side. We include an analysis of a second EXP dataset (green squares) acquired at $R_\lambda = 961$ in order to illustrate typical variation in large n behavior. The standard deviation in the experiment is approximately constant for about two orders of magnitude for $n > 10^8$, or equivalently for more than 10^5 turnover times, while that in DNS shows a -0.31 ± 0.04 power-law decay for $n > 3 \times 10^{12}$, as indicated by the solid line. The sample size in DNS cannot be easily translated to turnover time scales. The dashed line in panel (a) corresponds to the $-1/2$ scaling of random noise.

FIG. 4. Ratio of logarithmic local slopes of S_6 and S_2, $\zeta_{6,2}(r) \equiv d[\log S_6(r)]/d[\log S_2(r)]$ versus spatial separation r normalized by Kolmogorov scale η. Error bars indicate standard error obtained from temporal fluctuations of local slopes. Data from experiment (open circles) and the isotropic sector of DNS (solid line) are compared with the p-model (dash-dot line) of Meneveau and Sreenivasan [19], She-Leveque model (dashed line) [20] and that by Yakhot (dotted line) [21]. Horizontal line at $\zeta_{6,2} = 3$ corresponds to self-similar non-intermittent scaling [5]. Inset shows a blow-up of the inertial range and to either side of it to highlight differences between EXP and DNS.

the isotropic sector from DNS could arise from the fact that the former is not projected onto the isotropic sector. Indeed, similar one-dimensional cuts in DNS shown in Fig. 2(c) behave differently along different directions beyond $r/\eta = 100$ with that along $\hat{\mathbf{r}} = (0,0,1)$ matching the EXP data closely in the inertial range. Another possible reason for the mismatch might be that EXP relies on Taylor's frozen flow hypothesis [28] while the DNS data do not. Finally, one cannot exclude non-universal and Reynolds-number-independent effects induced by different forcing mechanisms [29].

We compare $\zeta_{4,2}$ in Fig. 2(a) with three different phenomenological models. While the p-model of Meneveau and Sreenivasan with the parameter p set to their value of 0.7 [19] compares favorably with EXP, the model by Yakhot [21, 30] closely matches DNS. The She-Leveque prediction [20] lies in between EXP and DNS, being closer to the latter than the former. A similar comparison of $\zeta_{4,2}$ from EXP and DNS with other inertial range models [31–33], although not shown here, reveals that the agreement is qualitatively similar to those shown in Fig. 2.

We now assess in Fig. 2 the r-dependent inertial range oscillations modulating the power-law expectations of Eq. 1, which is the feature to which Ref. [12] drew at-
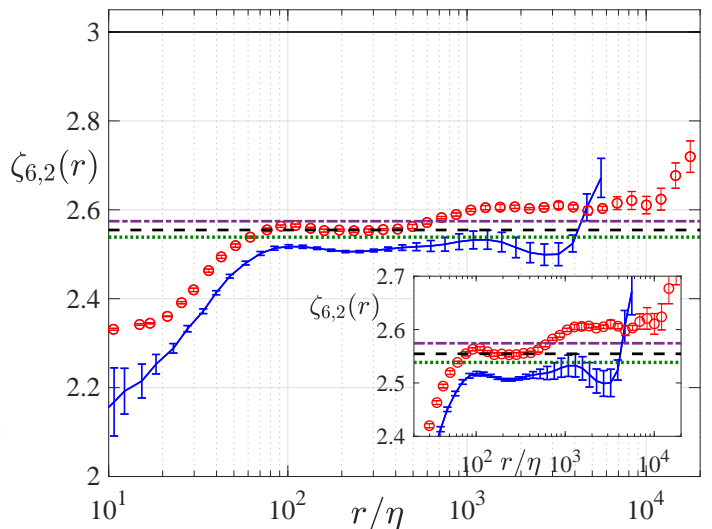
tention. Noting that the power-law behavior of Eq. 1 is expected to truly hold only at sufficiently large R_λ and as sample size $n \to \infty$, and that real systems such as the ones examined here are obviously at finite Reynolds numbers, we measure the oscillation amplitude for EXP and DNS and plot their standard deviations as functions of their respective sample size n in Fig. 3. EXP and DNS show different behaviors, with EXP suggesting a saturation at a small but finite value at even the large sample sizes considered here, while DNS exhibit a power-law decay with the sample size, even though care must be taken because of the short scaling range. Furthermore, the departure from a pure power law can have different origins depending on whether we are close to the viscous scale or to the integral scale. For example, while viscous effects are much less affected by statistical sampling, large scale properties can be less stable because of lack of statistics in DNS and some sustained low-level forcing of a different kind in EXP. The differences in the data might also result from differences in the averaging procedures in the two instances or to differences in the extent of the two datasets. We recall that the standard deviation for random noise varies as $n^{-1/2}$ with sample size.

The differences that exist between EXP and DNS in the inertial range in Fig. 2 persist at higher orders. Figure 4 shows $\zeta_{6,2} \equiv d[\log S_6]/d[\log S_2] = \zeta_6/\zeta_2$ as a

function of scale r with a focus in the inertial range, $r/\eta \in (100, 1000)$. K41-similarity [5] would correspond to $\zeta_{6,2} = 3$. Both EXP and isotropic DNS show roughly double the deviation from K41-similarity at the level of $\zeta_{6,2}$ than that at $\zeta_{4,2}$ (the increased departure being a characteristic of intermittency), and exhibit qualitatively similar behavior including the persistence of differences between EXP and DNS (see inset of Fig. 4). In the case of $\zeta_{6,2}$ the She-Leveque model [20] seems to agree somewhat better with EXP than the p-model, which underpredicts the level of intermittency. All three models appear to under-predict the inertial range intermittency of the DNS for $\zeta_{6,2}$.

In summary, we have examined the commonly held belief that the non-universal large-scale and viscous effects are forgotten to yield universal statistics well inside the inertial range. In particular, we compared turbulence data from simulations and experiments at similar Reynolds numbers to examine if power-law scaling prevails in the inertial range and, if it does, to what extent the assumed universality [34, 35] holds for structure functions. We paid particular attention to the likelihood of small oscillations in the inertial range, which could arise from large scales in the flow or from the viscous effects. We found that the latter effects in the exponent ratios persist up to $r/\eta \sim 80$ (although this precise number may vary with the context). For larger scale separations and up to $r/\eta \sim 1000$ scaling properties are close to a pure power-law with superposed small oscillations that decrease with increasing scale and Reynolds number; the oscillation amplitudes seem to decay continually with sample size in DNS; in EXP, however, after a conspicuous decay initially, they have a sustained presence of about 4 parts in 1000 even for very large sample sizes. A small but detectable mismatch between DNS and EXP data is measured at all scales, indicating a strong persistence of some large-scale non-universal properties to be further understood. On the question of universality, we confirmed that the scaling exponent ratios depart considerably from the K41 prediction [1, 2] and that existing phenomenological models do not account for all aspects of the observed small-scale non-universalities. These subtle findings have been possible because of the unprecedented combination of high sample sizes and high Reynolds numbers in both DNS and EXP. We are entering an era where scaling laws in turbulent flows can be assessed within a few percent of error and scale-by-scale over two or more decades.

ACKNOWLEDGMENTS

* krs3@nyu.edu

[1] A. S. Monin and A. M. Yaglom. *Statistical Fluid Mechanics* (MIT Press, Cambridge, MA, 1975), Vol. 2.

[2] U. Frisch, *Turbulence – The Legacy of A. N. Kolmogorov* (Cambridge University Press, Cambridge, UK, 1995).

[3] K. R. Sreenivasan and R. A. Antonia, The phenomenology of small-scale turbulence, Annu. Rev. Fluid Mech. **29**, 435 (1997).

[4] T. Ishihara, T. Gotoh and Y. Kaneda, Study of high-Reynolds number isotropic turbulence by direct numerical simulation, Annu. Rev. Fluid Mech. **41**, 165 (2009).

[5] A. N. Kolmogorov, Dissipation of energy in locally isotropic turbulence, Dokl. Akad. Nauk. SSSR **32**, 16–18 (1941).

[6] K. R. Sreenivasan and B. Dhruva, Is there scaling in high-Reynolds-number turbulence? Prog. Theor. Phys. Suppl. **130**, 103–120 (1998).

[7] N. Goldenfeld, Lectures on phase transitions and the renormalization group, Frontiers Phys. **85**, 279-282 (1992).

[8] A. Barabási, The origin of bursts and heavy tails in human dynamics, Nature **435**, 207211 (2005).

[9] D.W. Sims, E.J. Southall, N.E. Humphries, G.C. Hays, C.J.A. Bradshaw, J.W. Pitchford, A. James, M.Z. Ahmed, A.S. Brierley, M.A. Hindell, D. Morritt, M.K. Musyl, D. Righton, E.L.C. Shepard, V.J. Wearmouth, R.P. Wilson, M.J. Witt, and J.D. Metcalfe, Scaling laws of marine predator search behaviour, Nature **451**, 10981102 (2008).

[10] M. P. H. Stumpf and M. A. Porter, Critical truths about power laws, Science **335**, 665 (2012).

[11] G. L. Eyink, Besov spaces and the multifractal hypothesis, J. Stat. Phys. **78**, 353 (1995).

[12] M. Sinhuber, G.P. Bewley and E. Bodenschatz, Dissipative effects on inertial-range statistics at high Reynolds numbers, Phys. Rev. Lett. **119**, 134502 (2017).

[13] P. K. Yeung, X. M. Zhai and K. R. Sreenivasan, Extreme events in computational turbulence, Proc. Nat. Acad. Sci. **112**, 12633–12638 (2015).

[14] K. P. Iyer, K. R. Sreenivasan and P. K. Yeung, Reynolds number scaling of velocity increments in isotropic turbulence, Phys. Rev. E **95**, 021101(R) (2017).

[15] K. P. Iyer, K. R. Sreenivasan and P. K. Yeung, Scaling exponents saturate in three-dimensional isotropic turbulence, arXiv:2002.11900 (2020).

[16] S. Kurien and K. R. Sreenivasan, *Measures of anisotropy and the universal properties of turbulence* (Springer, Berlin, 2001), pp. 53–111.

[17] L. Biferale and I. Procaccia, Anisotropy in turbulent flows and in turbulent transport, Phys. Rep. **414**, 43–

164 (2005).

[18] K. P. Iyer, F. Bonaccorso, L. Biferale and F. Toschi. Multiscale anisotropic fluctuations in sheared turbulence with multiple states, Phys. Rev. Fluids **2**, 052602(R) (2017).

[19] C. Meneveau and K.R. Sreenivasan, Simple multifractal cascade model for fully developed turbulence, Phys. Rev. Lett. **59**, 1424 (1987).

[20] Z. S. She and E. Leveque, Universal scaling laws in fully developed turbulence, Phys. Rev. Lett. **72**, 336 (1994).

[21] V. Yakhot, Mean-field approximation and a small parameter in turbulence theory, Phys. Rev. E **63**, 026307 (2001).

[22] R. Benzi, S. Ciliberto, R. Tripiccione, C. Baudet and S. Succi, Extended self-similarity in turbulent flows, Phys. Rev. E **48**, R29-R32 (1993).

[23] R. Benzi, L. Biferale, R. Fisher, D. Q. Lamb and F. Toschi, Inertial range Eulerian and Lagrangian statistics from numerical simulations of isotropic turbulence, J. Fluid Mech. **653**, 221-244 (2010).

[24] U. Frisch and M. Vergassola, A prediction of the multifractal model: the intermediate dissipation range, Europhys. Lett. **14**, 439 (1991).

[25] C. Meneveau, Transition between viscous and inertial-range scaling of turbulence structure functions, Phys. Rev. E **54**, 3657 (1996).

[26] D. A. Donzis and K. R. Sreenivasan, The bottleneck effect and the Kolmogorov constant in isotropic turbulence, J. Fluid Mech. **657**, 171-188 (2010).

[27] C. Küchler, G. Bewley and E. Bodenschatz , Experimental Study of the Bottleneck in Fully Developed Turbulence, J. Stat. Phys. **175**, 617-639 (2019).

[28] Taylor, G.I, Statistical theory of turbulence, Proc. R. Soc. Lond. A Math. Phys. Sci. **151**, 421 (1935).

[29] V. Yakhot and D. Donzis, Emergence of multiscaling in a random-force stirred fluid, Phys Rev. Lett. **119**, 044501 (2017). V. Yakhot, Matching Conditions and High-Re Anomalies in Hydrodynamic Turbulence. arXiv:1812.02883 (2018)

[30] J. Schumacher, K. R. Sreenivasan and V. Yakhot, Asymptotic exponents from low-Reynolds-number flows, New J. Phys. **9**, 89–89 (2007).

[31] R. Benzi, G. Paladin, G. Parisi and A. Vulpiani, On the multifractal nature of fully developed turbulence and chaotic systems, J. Phys. A: Math. Gen. **17**, 3521-3531 (1984).

[32] D. P. Ruelle, Hydrodynamic turbulence as a problem in nonequilibrium statistical mechanics, Proc. Nat. Acad. Sci. **109**, 20344–20346 (2012).

[33] C. Eling and Y. Oz, The anomalous scaling exponents of turbulence in general dimension from random geometry, J. High Energ. Phys. **2015**, 150 (2015).

[34] E.-W. Saw, P. Debue, D. Kuzzay, F. Daviaud and B. Dubrulle, On the universality of anomalous scaling exponents of structure functions in turbulent flows. J. Fluid Mech. **837**, 657669 (2018).

[35] N. Reinke, A. Fuchs, D. Nickelsen and J. Peinke, On universal features of the turbulent cascade in terms of non-equilibrium thermodynamics, J. Fluid Mech. **848**, 117-153 (2018).